Spinal Cord Schistosomiasis: MR Imaging Appearance with Surgical and Pathologic Correlation

Sahar Saleem, Adel I. Belal, and Nasser M. El-Ghandour

BACKGROUND AND PURPOSE: Spinal cord involvement is a rare manifestation of schistosomiasis. We describe the MR imaging findings of spinal cord schistosomiasis in correlation with surgery and pathology.

METHODS: We report eight cases of spinal cord schistosomiasis. All patients were men (mean age, 16.7 years) with neurologic manifestations who had been referred for spinal MR imaging. In all cases, spinal masses were surgically removed. MR imaging findings were correlated with surgery and pathology.

RESULTS: MR imaging showed moderate expansion of the distal spinal cord in all cases. Abnormalities were isointense to cord in T1 and patchy hyperintense in T2-weighted spin-echo images ($n = 8$). Three forms of contrast enhancement were recognized: (1) intramedullary nodular ($n = 8$); (2) peripheral ($n = 8$); and (3) linear radicular ($n = 4$). Total gross surgical removal of masses by using the Cavitron ultrasonic surgical aspirator was possible in six cases. Diagnosis was established by identification of ova in histopathologic studies: *Schistosoma mansoni* ($n = 3$), *S hematobium* ($n = 1$), and uncertain species ($n = 4$). Intramedullary nodular enhancement was correlated to multiple schistosomiasis microtubercles. Peripheral enhancing lesions correlated to thickened leptomeninges infested by chronic granulomatous inflammatory cells and schistosoma eggs. Linear radicular enhancement correlated with thickened resected nervous roots infested by granulomatous cells and schistosoma eggs.

CONCLUSION: Multinodular intramedullary contrast enhancement of the distal cord enabled correct presumptive preoperative MR imaging diagnosis of spinal schistosomiasis in three cases. Accurate diagnosis, through recognition of its MR imaging appearance, allows early treatment and better prognosis of spinal cord schistosomiasis.

Schistosomiasis is a human trematode infection affecting at least 200 million people worldwide. The infection is endemic to Africa, South America, and most parts of Asia (1). The typical manifestations of schistosomiasis are urogenital, intestinal and hepatolienal (2), and involvement of other organs, especially the central nervous system, is uncommon (3).

Symptomatic spinal cord involvement is a rare but well-documented manifestation of schistosomiasis (4, 5). A nonspecific intramedullary expansion in the caudal spinal cord is the most common finding in conventional and computed myelography (6, 7). The literature concerning MR imaging of spinal cord schistosomiasis is scarce, and pathologically confirmed cases are mainly limited to isolated case reports (8–10). In this study, we report the MR imaging findings of eight surgically confirmed cases of spinal cord schistosomiasis and correlate them with surgical and pathologic data.

Methods

Patients

Eight male patients (age range, 6–43 years; mean $\pm$ SD, 16.7 ± 11.7 years; median, 13 years) presenting with neurologic manifestations (Table 1) were referred to our hospital for spinal MR imaging between January 1994 and June 2002. The duration of their complaint ranged from 2 to 18 months, with an average of 7 months. No fever or systemic illness was reported, except for hepatosplenomegaly in one patient (case 5). All patients came from areas where schistosomiasis is endemic and gave histories of repeated contact with Schistosoma-contaminated water.

In all patients, serum analysis showed no evidence of eosinophilia. Multiple stool and urine analysis in all patients was

TABLE 1: Clinical, surgical, and pathologic findings, and neurologic outcome of eight patients with spinal cord schistosomiasis

Case	Age (years)	Autonomic Dysfunction (Sphincteric)	Leg Weakness	Limb Pain	Back Pain	Surgery: Mass Resection	Pathology	Neurological Outcome
1	7	−	+	+	−	Total	*S mansoni*	Improved
2	9	+	+	−	−	Total	*S hematobium*	Improved
3	6	+	+	−	−	Total	Nonspined ova	Improved
4	11	+	+	−	+	Total	*S mansoni*	Stabilized
5	27	−	−	+	−	Total	*S mansoni*	Improved
6	15	+	+	−	−	Total	Nonspined ova	Improved
7	16	−	+	−	+	Partial	Deformed ova	Improved
8	43	−	+	+	+	Partial	Deformed ova	Stabilized

Note.—*S* indicates *Schistosoma*; +, present; −, absent.

TABLE 2: MRI findings in eight patients with spinal cord schistosomiasis

Case	Site of Spinal Abnormality: Cord—Cauda Equina	Signal Pattern		Contrast Enhancement		
		T1-Weighted SE	T2-Weighted SE	Intramedullary Nodular	Peripheral	Radicular
1	T12–L2	Isointense	Hyperintense	+	+ C	+
2	T12–L1	Isointense	Hyperintense	+	+ C	−
3	T12–L3	Isointense	Hyperintense	+	+ C	+
4	T11–T12	Isointense	Isointense	+	+ A, P	−
5	T9–L1	Isointense	Isointense	+	+ A	−
6	T12–L1	Iso-, hypointensities	Iso-, hypointensities	+	+ A	−
7	T11–T12	Isointense	Isointense	+	+ A	+
8	T10–L1	Iso-, hypointensities	Iso-, hypointensities	+	+ A	+

Note.—A indicates anterior; C, circumferential; L, lumbar; P, posterior; SE, spin echo; T, thoracic; +, present; −, absent.

negative for Schistosoma species ova. CSF studies were available for four patients (cases 1, 2, 5, and 7) and showed a mild increase in total protein level (35–40 mg/dL) as well as mild lymphocytic pleocytosis (5–8 cells/mm³) in all cases. Eosinophils were not observed in the CSF of any of our patients. Myelography and CT myelography were available in four patients, and all showed moderate nonspecific expansion of the distal spinal cord and conus medullaris.

MR Imaging Technique

All patients underwent MR imaging of the dorso-lumbar spine. Five patients were examined by using 1.5T, and three were performed by using 1.0T, MR units. Surface coils were used for all patients.

Spin-echo (SE) T2-weighted images were obtained in sagittal and axial planes. Standard T2-weighted SE images were taken in five cases (TR range, 1880–2550 ms; TE range, 20–38/90–120 ms, to obtain dual echoes, the first being the proton density image). Fast T2-weighted SE imaging was performed for the other three patients by using a TR of 2500 ms and TE of 120 ms. All patients were studied with T1-weighted TR/TE (400–600/20–25 ms) in sagittal, axial, and coronal planes before and after receiving 0.1 mmol/kg gadolinium injected intravenously over the course of 1 minute.

In the sagittal plane, 4-mm section-thickness images with interslice gap of 0.4 mm were obtained through the cord by using 190–260 mm fields of view [FOVs]. In the axial scans, 4–6-mm section-thickness images with interslice gap of 0.4 mm were obtained in the region of interest by using 160–200-mm

FOVs. The number of signal intensity averages (NSAs) ranged from 2 to 6 in T1-weighted images and were from 1 to 4 in T2-weighted images. The matrix used was usually 307 × 512 in the sagittal plane and 190 × 512 in the axial plane.

MR imaging of intraspinal lesions was characterized by their location, contour, signal intensities, and pattern of contrast enhancement. All MR images were evaluated by the two radiologists in this study, and the final decisions were reached by consensus.

All the patients were operated upon with general anesthesia in the prone position. Laminectomy was performed at the site of the lesion, as determined by the MR images, followed by a midline dural incision. A microsurgical procedure was used in all cases with the Cavitron ultrasonic surgical aspirator (CUSA) for lesion removal.

Gross and microscopic pathologic examinations of the surgical specimens were part of the routine clinical service. Multiple histopathologic sections were taken stained with hematoxylin and eosin (H & E).

Results

MR Imaging Results

MR images in all patients showed mild to moderate expansion of the distal spinal cord and conus medullaris in all cases (Table 2). The signal intensity abnormalities were mainly isointense to cord in T1-weighted images and patchy hyperintense in T2-

Fɪɢ 1.   Localization of spinal cord schistosomiasis. MR imaging of dorso-lumbar spine of case 3.

A, Sagittal T1-weighted SE (TR/TE 530/20 ms) image shows moderate expansion of the distal cord and conus medullaris (*arrow*). The lesion is isointense to the cord.

B, Sagittal T2-weighted SE (TR/TE 5800/95 ms) image. The lesion has heterogeneous hyperintense signal intensity (*arrow*).

C, Coronal T1-weighted SE MR images (TR/TE 520/20 ms) shows the expanded distal cord and conus medullaris (*arrow*).

D, Postcontrast coronal image, in which the lesion is well delineated by contrast enhancement (*arrow*). Note the associated linear enhancement of cauda equina nerve roots (*arrowhead*).
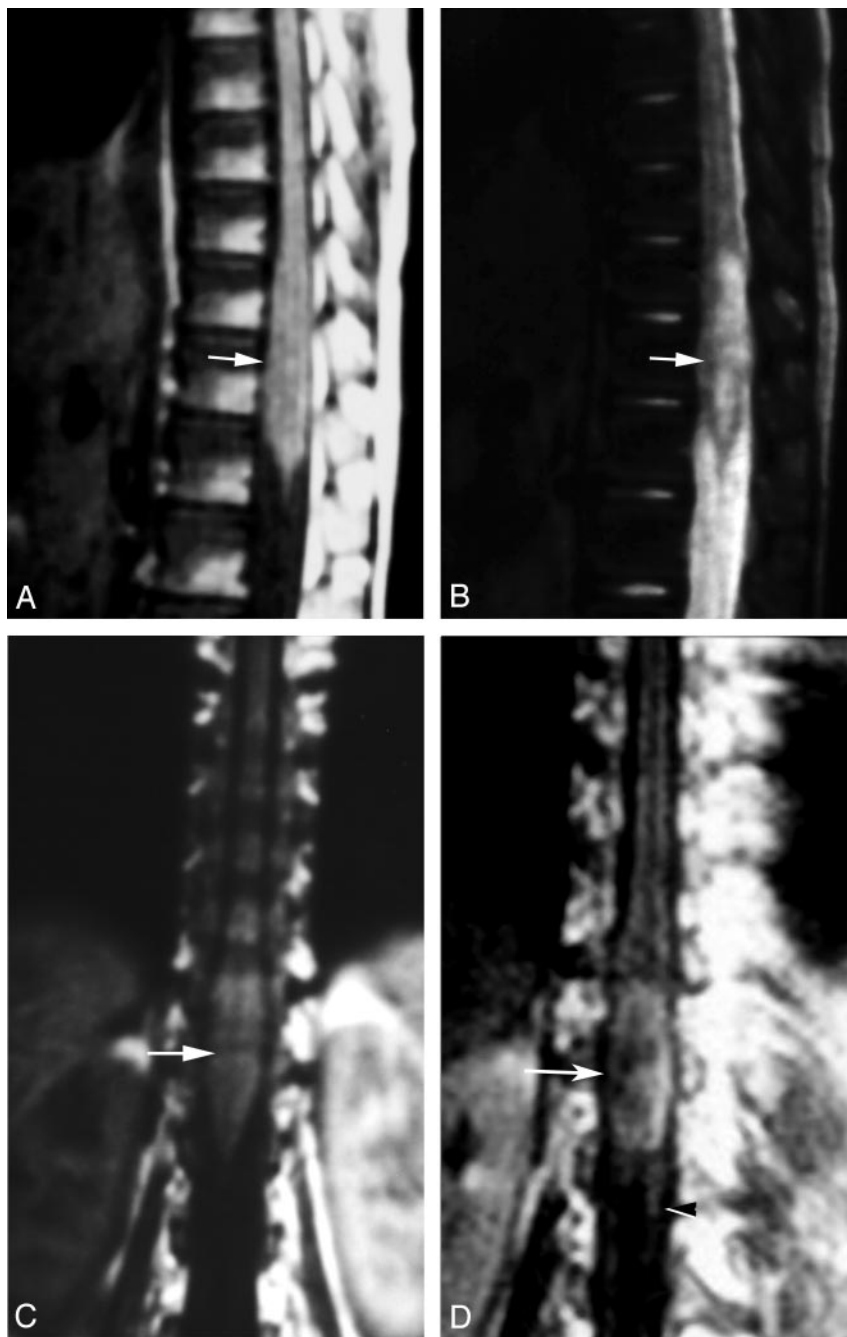
weighted images (Fig 1*A* and -*B*). Abnormal intraspinal contrast enhancement was detected in all patients and enabled accurate delineation of the pathologic process (Fig 1*C* and -*D*). The highest and the lowest levels of abnormalities were thoracic (T) nine and lumbar (L) three, respectively. The length of the involved cord segments ranged between 2 and 4.5 (average, 2.5) vertebral heights.

Three different forms of abnormal intraspinal contrast enhancement were recognized: (A) intramedullary nodular enhancement (*n* = 8). In seven patients, the nodules were multiple and varied in size from minute foci of <3 mm in diameter, to larger nodules up to 20 mm in long axis (Fig 2*A*). One patient had a solitary localized masslike enhancing nodule, measuring 15 mm

in its long axis (Fig 3). (B) Peripheral enhancing lesions on the cord surface (*n* = 8). These lesions were located mainly on the anterior aspect of the cord, best identified in axial plane (Fig 4*B* and -*C*). (C) Enhancing thickened nerve roots and cauda equina (*n* = 4). Irregular thick linear enhancement was noted along the course of the cauda equina nerve roots (Fig 5).

In addition, a small reactional syrinx with nonenhancing walls was detected proximal to the lesion in one patient (case 8).

Surgical Findings

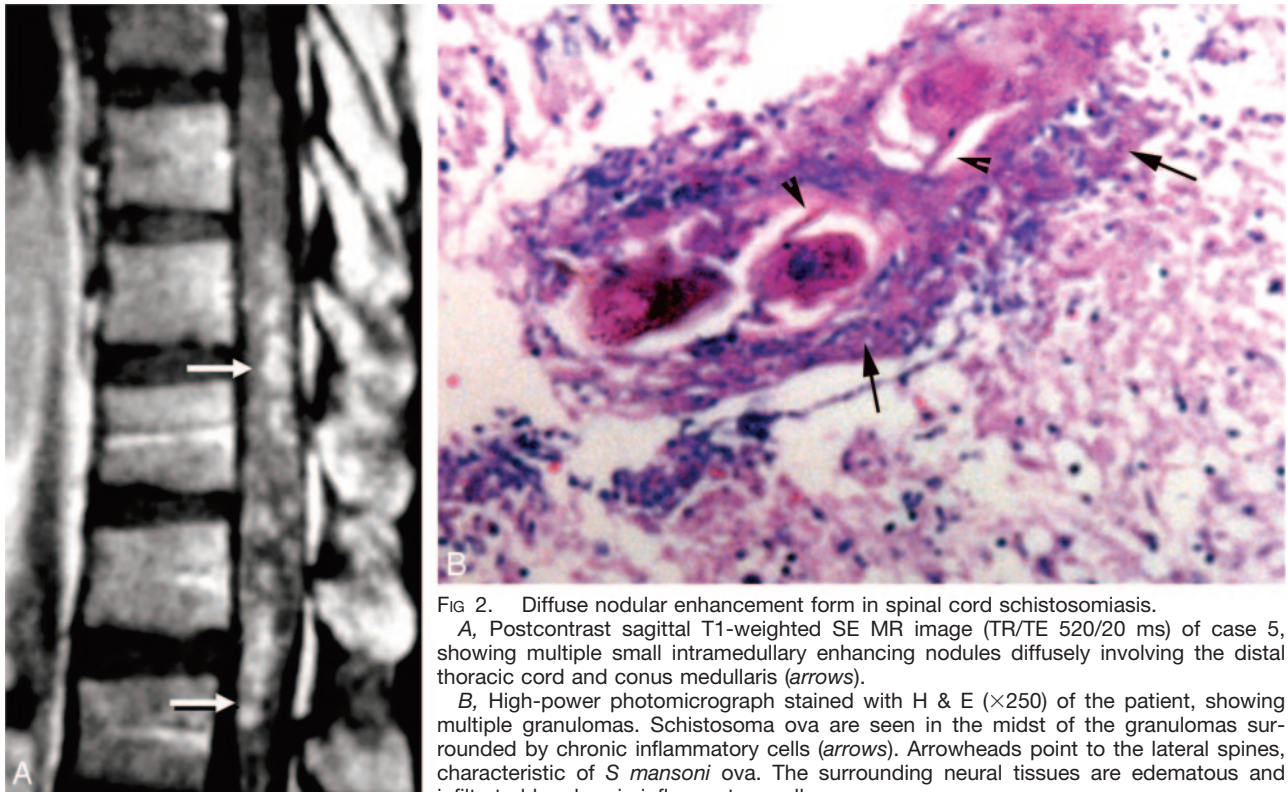Intraoperatively, expansion of the distal cord and conus medullaris was seen in all cases. The cord

Fɪɢ 2.   Diffuse nodular enhancement form in spinal cord schistosomiasis.
A, Postcontrast sagittal T1-weighted SE MR image (TR/TE 520/20 ms) of case 5, showing multiple small intramedullary enhancing nodules diffusely involving the distal thoracic cord and conus medullaris (*arrows*).
B, High-power photomicrograph stained with H & E (×250) of the patient, showing multiple granulomas. Schistosoma ova are seen in the midst of the granulomas surrounded by chronic inflammatory cells (*arrows*). Arrowheads point to the lateral spines, characteristic of *S mansoni* ova. The surrounding neural tissues are edematous and infiltrated by chronic inflammatory cells.

masses were grayish in color, irregular in shape with a nodular appearance. They were firm in consistency and relatively avascular. The masses gave a gritty sensation during excision. Total gross removal of the spinal cord masses was attempted by using the CUSA. In six cases (75%), total gross removal of the spinal cord masses was possible because of the presence of a good plane of cleavage between these lesions and the surrounding spinal cord tissue. Only partial resection of the spinal masses in the other two cases was possible. Irregular thickening of the meninges overlying the cord masses was noted in all cases (100%), and the irregular nodular appearance of the roots of cauda equina was noted in four cases (50%).

Pathologic Results

The gross surgical pathologic specimens included grayish soft tissue fragments. Sections of the excised masses with H & E showed infiltration of the spinal cord by multiple Schistosomal granulomas. Schistosoma ova with refractile shell were seen in the midst of the granulomas, surrounded by fibroblasts, eosinophils, lymphoplasma cells, and macrophage histiocytes. The gray and white matter were affected equally. Granulomas were mainly present beside blood vessels. There were areas of reactive astroglial tissues and fibrosis in all cases with variable attenuation. Infiltration was seen peripherally in the meninges in all cases and in the resected spinal nerve roots in four cases. Schistosomal ova were identified in all cases. *S mansoni* ova were detected in three cases, recognized by their characteristic lateral spines (Fig 2*B*).

S hematobium ova were detected in one patient; they were identified by their central spines (Fig 4*D*). In the other four cases with Schistosomes, the species could not be determined, either because the histologic slides did not coincide with any spined ova (*n* = 2) or the ova were deformed and calcified (*n* = 2).

MR Imaging Findings in Correlation with Surgical and Pathologic Data

The affected spinal cord segments identified by MR imaging (*n* = 8), were grayish in color, had a nodular appearance, and were gritty during surgical excision. The hypointense signals detected in two cases were correlated with areas of attenuated fibrosis (Fig 3*B*). Intramedullary nodular contrast enhancement was correlated to multiple schistosomiasis microtubercles found in histopathologic sections of all patients. Schistosoma ova were seen surrounded by granulomatous chronic inflammatory cells: eosinophils, lymphoplasma cells, and macrophage histiocytes. The peripheral enhancing lesions in MR imaging were correlated to thickened infested leptomeninges at surgery and in pathology. The leptomeninges showed the chronic granulomatous inflammatory cells, as well as the presence of schistosoma eggs. The resected nerve roots in the four MR-positive cases were thickened by a chronic granulomatous inflammatory process surrounding schistosoma eggs.

Postoperative Outcome and Follow-Up

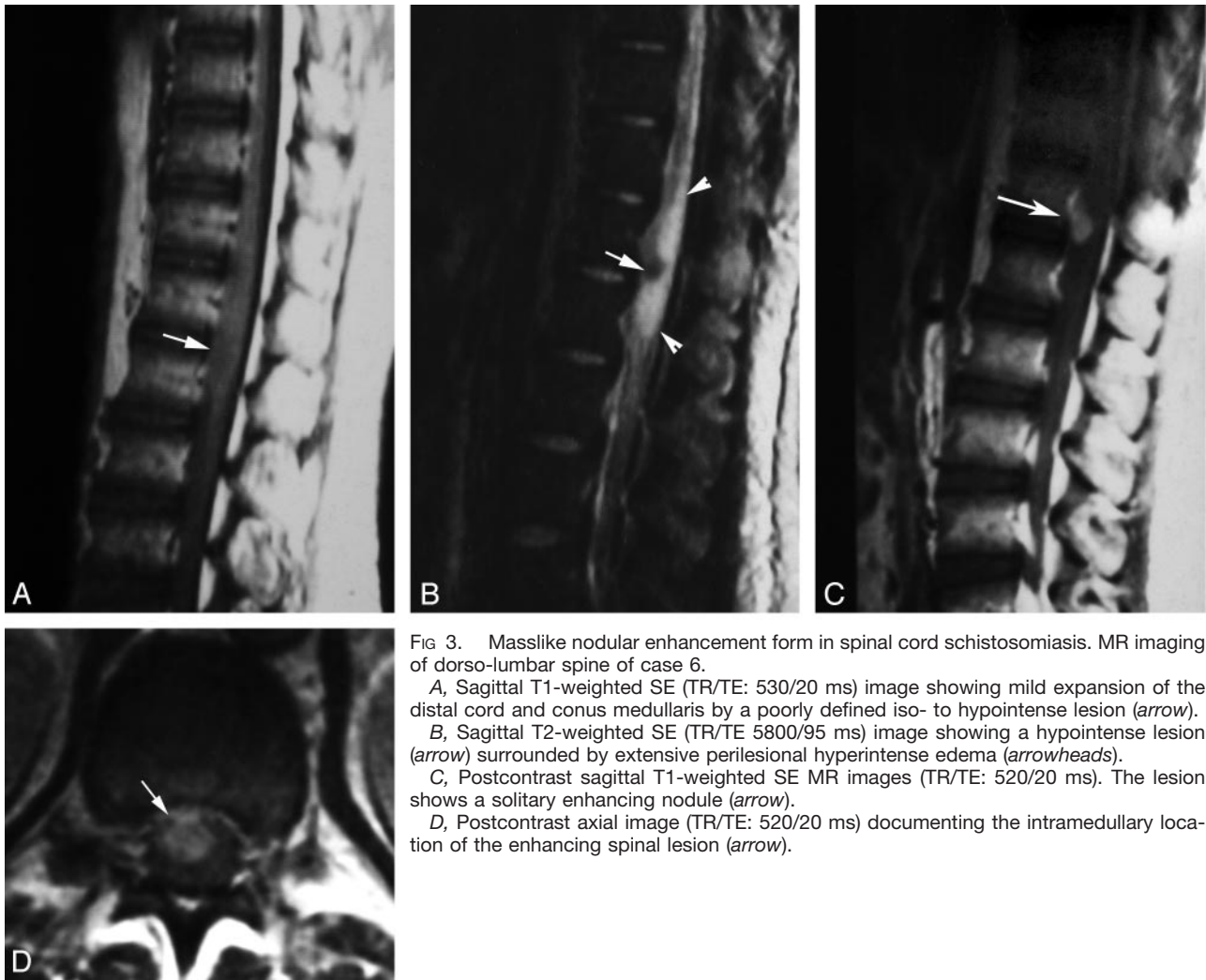Postoperative course was uneventful in all the cases. Praziquantel, a specific antischistosomiasis

FIG 3.   Masslike nodular enhancement form in spinal cord schistosomiasis. MR imaging of dorso-lumbar spine of case 6.

A, Sagittal T1-weighted SE (TR/TE: 530/20 ms) image showing mild expansion of the distal cord and conus medullaris by a poorly defined iso- to hypointense lesion (*arrow*).

B, Sagittal T2-weighted SE (TR/TE 5800/95 ms) image showing a hypointense lesion (*arrow*) surrounded by extensive perilesional hyperintense edema (*arrowheads*).

C, Postcontrast sagittal T1-weighted SE MR images (TR/TE: 520/20 ms). The lesion shows a solitary enhancing nodule (*arrow*).

D, Postcontrast axial image (TR/TE: 520/20 ms) documenting the intramedullary location of the enhancing spinal lesion (*arrow*).

treatment, was given to all patients as a single dose of 40 mg/kg body weight for 3 successive days. Dexamethazone was also given in the dosage of 0.5–1 mg/kg body weight per day in two divided doses for 2 days, which was gradually tapered to 0.25 mg/day to cover the postoperative course for an average 1-week duration. Clinical outcomes are reported in Table 1.

Discussion

Schistosomiasis (Bilharziasis) is caused by infestation of trematode Schistosoma, first discovered by Theodore Bilharz in 1851 in a postmortem study at Kasr Al-Ainy Hospital, in Cairo, Egypt (2). Schistosomiasis, in fact, was known in ancient Egypt. The disease was described in the Papyrus of Kahun (1852 B.C.), and Schistosoma ova were found in Egyptian mummies (11, 12). Three species of schistosomes infest man: *S hematobium, S mansoni,* and *S japonicum,* which differ in their geographic distribution; however, schistosomiasis is spreading to new areas because of travel and migration of infected populations (13).

According to the different predilection of each species, the adult Schistosoma worms live in vesical and mesenteric veins. A female Schistosoma worm lays 200–2000 ova daily, which are usually expelled in urine and stool (2, 14). Spinal cord schistosomiasis is an "ectopic" lesion in that the vessels of the spinal cord are not generally used by the adult worm or ovum (15). The possible routes for spinal involvement are the retrograde venous embolization of Schistosomal ova or less likely in situ deposition of ova by adult worms showing anomalous migration into the spinal vessels (16).

The reported prevalence of spinal cord schistosomiasis is low with <100 cases reported in the literature (7, 9, 17). Some authors believe that spinal cord schistosomiasis is not rare but is, in fact, an underreported condition (3, 7, 9, 17). All reported patients with spinal cord schistosomiasis potentially have been exposed to infestation. Worldwide, *S mansoni* is the most frequent cause of Schistosomal myelopathy (3, 18) and was responsible for three of our four cases in which the species could be determined.

A unique clinical profile is seen in this disease (3, 16, 19–21), in which young men present with lumbar pain (75%), often of a radicular nature, soon followed by rapid progression of weakness of the lower limbs (87.5%), and associated with autonomic dysfunction,
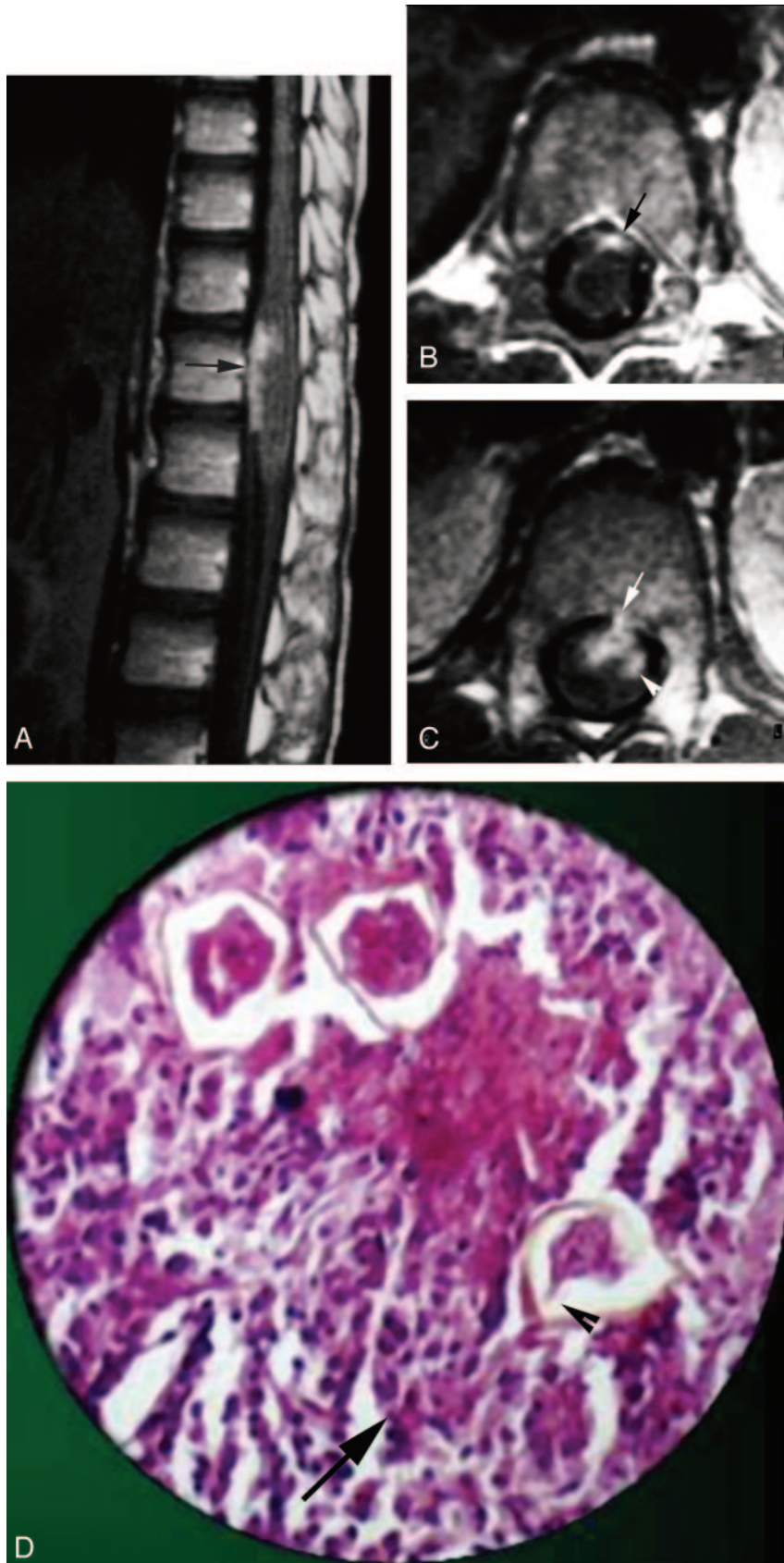
FIG 4.   Peripheral enhancement form of spinal cord schistosomiasis. MR imaging of dorso-lumbar spine and histopathologic slide of case 2.

A, Postcontrast sagittal image (TR/TE 520/20 ms) shows peripheral and intramedullary enhancing lesions on the anterior surface of the distal spinal cord (*arrow*).

B, Postcontrast axial image (TR/TE 520/20 ms), clearly showing the peripheral (meningeal) enhancement on the anterior surface of the cord (*arrow*).

C, Postcontrast axial image, which is inferior to that shown in *B*, shows a small peripheral enhancing lesion on the anterior cord surface (*arrow*) in association with an underlying intramedullary cord enhancement (*arrowhead*).

D, High-power photomicrograph stained with H & E (×250) showing infiltration of the resected neural tissues by chronic inflammatory cells (*arrow*) surrounding multiple schistosoma ova. One of the ova shows the terminal spine characteristic of *S hematobium* (*arrowhead*).
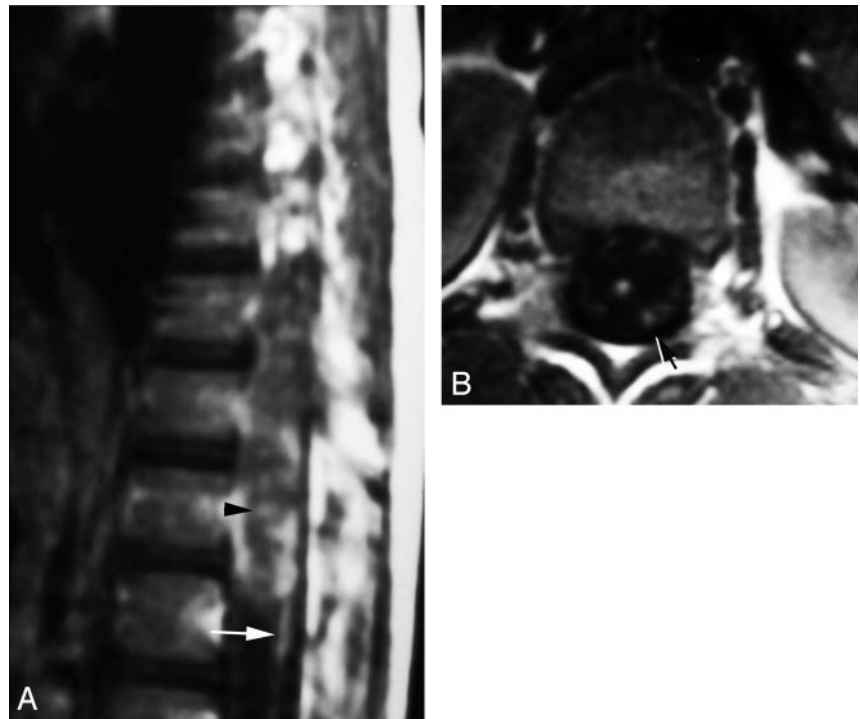
particularly bladder dysfunction (50%). The increased prevalence in young male patients in this disease (3, 19–21) may be explained by the social background, because men are more likely to be exposed to contaminated water than women from early childhood, during swimming, and in their youth,

working as farmers. Spinal schistosomiasis is often unassociated with visceral involvement (21), and in our study seven patients (87.5%) had no other manifestations of Schistosomal infection.

Spinal cord schistosomiasis has a spectrum of severity ranging from asymptomatic egg lying in the spinal cord, at one end of the spectrum, to a devastating acute transverse myelitis with hemorrhage and necrosis, at the other. Most cases occupy an intermediate position with granuloma formation and varying degrees of tissue damage. The concept applies not only to different patients, but also to the same patient at different stages of the disease (3). All the cases in our study were of the common granulomatous type. Granuloma is the better-defined entity of the disease because it is diagnosed following operation and biopsy. Transverse myelitis is seldom proved, and its diagnosis depends on circumstantial evidence (19), whereas asymptomatic deposition of ova in the cord is demonstrated only at necropsy (16).

CSF analysis reflected an inflammatory pattern characterized by a mild increase in the total protein concentration and pleocytosis. Eosinophils were not found in any of our patients. Although the presence of eosinophils in the CSF can contribute to the diagnosis of spinal schistosomiasis, it is reported only in 40% of patients and is nonspecific, because this cell can be seen in several other conditions (2, 7).

Myelographic findings (conventional and computed) in spinal cord schistosomiasis are nonspecific; moreover, a normal myelogram does not exclude the diagnosis (7, 22). The myelographic findings in this study showed nonspecific intramedullary expansion of the distal cord and conus medullaris.

MR imaging studies describing pathologically confirmed cases of spinal cord schistosomiasis in literature is scarce and is mainly individual case reports (17, 18, 23). The spinal abnormalities in our cases were located in the conus medullaris and the lower thoracic cord, the highest being at T9. Of the confirmed cases of Schistosomal myelopathy reported, the disease was less common at levels higher than T11 (19). This very consistent localization in the lower cord and conus region is explained by the free anastomosis between pelvic veins and the valveless vertebral venous plexus, as well as between the hemorrhoidal and systemic veins (6, 16)

The signal intensity pattern of the expanded cord segment was isointense to the cord parenchyma in T1 with heterogeneous hyperintense signal intensity in T2-weighted images. This pattern was also noted in a previous study (24). The low-signal-intensity areas correlated with attenuated fibrosis in two of our cases. The small reactive syrinx in one patient was also described in a previous report (22).

Previous case reports of the MR imaging findings associated with spinal schistosomiasis have described variable enhancement patterns by using nonspecific terms such as "heterogeneous" (17, 25), spotty (9, 26), or nodular enhancement (27). In this study, we described three different forms of contrast enhancement; intramedullary nodular, peripheral, and radicular forms.

The nodular intramedullary enhancement was linked to the pathologic finding of multiple granulomata, each surrounding one or more ova. Diffuse spinal cord schistosomiasis has been described elsewhere (14, 28). Large intraspinal Schistosomal granulomas, closely resembling gliomas macroscop-

ically, were also reported (29, 30). One of our cases showed a solitary enhancing masslike nodule.

The peripherally enhancing lesions seen in all patients represented infested meninges. It was noted in previous works (14, 17), as well as in the present study, that the meningeal granulomatous reaction is greatest anteriorly.

Abnormal contrast enhancement of the thickened cauda equina nerve roots represented radicular infestation in four (50%) of our cases. Radicular infestation was described in association with the intramedullary granulomatous type (31), but not as the sole feature of spinal cord schistosomiasis (16).

The differential diagnoses of spinal cord schistosomiasis include neoplastic and other non-neoplastic cord lesions. Like most non-neoplastic cord lesions (transverse myelitis, multiple sclerosis, and infarction), spinal schistosomiasis shows less anatomic distortion than intramedullary cord tumors. Schistosomal myelopathy, however, differs from other causes of myelitis in that it commonly affects the lower cord, whereas transverse myelitis commonly affects the midthoracic region (7, 8, 22). Multinodular intramedullary contrast enhancement of the distal cord enabled correct presumptive preoperative MR imaging diagnosis of spinal schistosomiasis in three cases in this study. The association of enhancing peripheral lesions with the intramedullary nodules seen in all cases could represent a possible MR imaging pattern of this disease.

In a study of three cases with nonpathologically confirmed CNS lesions assumed to be due to schistosomiasis, Sanelli et al described a central linear enhancement surrounded by multiple enhancing nodules (27). They considered this pattern to be specific and unique for this disease; however, we did not encounter this pattern in this study or in our review of previous reports in the literature.

Total resection of the spinal masses was attempted in all patients in this study. Some clinicians (3, 32), however, argue against the need for biopsy to establish the diagnosis. It has been suggested that, if the diagnosis of spinal cord schistosomiasis can be made on the basis of clinical presentation and imaging evidences, medical therapy alone with imaging follow-up would be an appropriate and less-invasive treatment (17). Other clinicians believe, as do we, that most of the patients with spinal cord schistosomiasis will benefit from surgery by partial resection of the lesion, with the additional use of antischistosomal drugs. Corticosteroids may also be helpful (4, 16, 28). The favorable outcome of six cases (75%) in this study was attributed to early surgical and medical treatment before irreversible damage occurred.

Conclusion

Schistosomiasis of the spinal cord should be considered in the differential diagnosis of lesions affecting the lower thoracic cord-conus medullaris-cauda equina in patients from endemic areas with history of exposure to Schistosomal infestation. MR imaging can reveal the true extent of the disease and can suggest the diagnosis through recognition of its signal intensity changes and enhancement forms. Accurate diagnosis allows early treatment and results in better prognosis of spinal cord schistosomiasis.

Acknowledgments

References

1. World Health Organization. **Public health impact of schistosomiasis.** *Bull WHO* 1993;71:623–657
2. Mahmoud AA. **Trematodes (schistosomiasis, other flukes).** In: Mandell GL, Douglas RG, Bennet JE, eds. *Principles and practice of infectious diseases.* 2nd ed. New York: Wiley Medical;1985: 1573–1579
3. El Banhawy A, Elwan O, Taher Y. **Bilharzial granuloma of the conus medullaris and cuada equina.** *Paraplegia* 1972;10:172–180
4. Luyendijk W, Lindeman J. **Schistosomiasis (Bilharziasis) mansoni of the spinal cord simulating an intramedullary tumor.** *Surg Neurol* 1975;4:457–460
5. Dar J, Zimmerman RR. **Schistosomiasis of the spinal cord.** *Surg Neurol* 1977;8:416–418
6. Herskowitz A. **Spinal cord involvement with *Schistosoma mansoni*: case report.** *J Neurosurg* 1972;36:494–498
7. Haribhai HC, Bhigjee AI, Bill PLA, et al. **Spinal cord schistosomiasis.** *Brain* 1991;114:709–726
8. Selwa ML, Brunberg JA, Mandell SH, Garofalo EA. **Spinal cord schistosomiasis: a pediatric case mimicking intrinsic cord neoplasm.** *Neurology* 1991;41:755–757
9. Ueki KU, Parisi JE, Onofrio BM. ***Schistosoma mansoni* infection involving the spinal cord: case report.** *J Neurosurg* 1995;82: 1065–1067
10. Leusen HV, Perquin WVM. **Spinal cord schistosomiasis.** *J Neurol Neurosurg Psychiatry* 2000;59:690–691
11. Contis G, David AR. **The epidemiology of Bilharzia in ancient Egypt: 5000 years of Schistosomiasis.** *Parasitol Today* 1996; 12:253–255
12. Miller RL, Armelagos GJ, Ikram S, et al. **Palaeoepidemiology of Schistosoma infection in mummies.** *BMJ* 1992;304:555–556
13. Winsberg GR, Moriearty P, Yoggore M. **Schistosomiasis in Chicago.** *Am J Epidemiol* 1974;100:324–332
14. Marcial-Rojas RA, Fiol RE. **Neurologic complications of schistosomiasis: review of the literature and report of two cases of transverse myelitis due to *S. mansoni*.** *Ann Intern Med* 1963;59:215–230
15. Faust EC. **An inquiry into the ectopic lesions in schistosomiasis.** *Am J Trop Med* 1948;28:175–177
16. Ghaly AF, El-Banhawy A. **Schistosomiasis of the spinal cord.** *J Pathol* 1973;111:57–60
17. Silbergleit R, Silbergleit R. **Schistosomal granuloma of the spinal cord: evaluation with MR imaging and intraoperative sonography.** *AJR Am J Radiol* 1992;158:1351–1353
18. Norfray JF, Schlachter LL, Heiser WJ, et al. **Schistosomiasis of the spinal cord.** *Surg Neurol* 1978;9:68–71
19. Consnett JE, Van Dellen JR. **Schistosomiasis (Bilharzia) of the spinal cord: case reports and clinical profile.** *Q J Med* 1986;61:1131–1139
20. Scrimgeour EM. **Spinal cord disease due to *Schistosoma mansoni* successfully treated with oxamniquape.** *BMJ* 1984;289:625–626
21. Queiroz AC, Nucci A, Facure NO, Facure JJ. **Massive spinal cord necrosis in Schistosomiasis.** *Arch Neurol* 1979;36:517–519
22. Blunt SB, Boulton J, Wise R. **MRI in schistosomiasis of conus medullaris and lumbar spinal cord.** *Lancet* 1993;341:55–57
23. Leite CC, Souza AF, Valente M, et al. **Clinics in diagnostic imaging (52): spinal cord schistosomiasis.** *Singapore Med J* 2000;41:417–419
24. Peregrino AJ, Puglia PM, Bacheschi LA, et al. **Diagnosis of schistosomiasis of the spinal cord: contribution of magnetic resonance imaging and electroneuromyography.** *Arch Qneuropsiquiatr* 2002;60:597–602

25. Carod-Artal FJ, Vargas AP. **Myelopathy due to *Schistosoma mansoni*: a description of two cases and review of the literature.** *Rev Neurol* 2004;39:137–141
26. Nobre V, Silva CS L, Ribas JG, et al. **Schistosomal myeloradiculopathy due to *Schistosoma mansoni*: report on 23 cases.** *Mem Inst Oswalso Cruz Rio de Janeiro* 2001;96(suppl):137–141
27. Sanelli PC, Lev MH, Gonzalez RG, Schaefer PW. **Unique linear and nodular MR enhancement pattern in schistosomiasis of the central nervous system: report of three patients.** *Am J Radiol* 2001;177:1471–1474
28. Scrimgeour EM, Gajdusek DC. **Involvement of the central nervous system in *Schistosoma mansoni* and *S. haematobium* infection: a review.** *Brain* 1985;108:1023–1038
29. Cohen J, Capildeo R, Rose FC. **Schistosomal myelopathy (letter).** *BMJ* 1977;2:1418
30. Bennett G, Provenzale JM. **Schistosomal myelitis: findings at MR imaging.** *Eur J Radiol* 1998;27:268–270
31. Ferrari TCA. **Involvement of central nervous system in the schistosomiasis.** *Mem Inst Oswaldo Cruz* 2004;99(suppl 1):59–62
32. Bird AV. **Spinal cord complications of Bilharziasis.** *S Afr Med J* 1965;39:158–162